XIX International Conference on Water Resources
CMWR 2012
University of Illinois at Urbana-Champaign
June 17-22, 2012

NUMERICAL FLOW EXPERIMENTS ON SAMPLES OF HETEROGENEOUS UNSATURATED POROUS MEDIA: UPSCALING THE PERMEABILITY-PRESSURE CURVE

Rachid Ababou[*], David Bailly[*†], Adrien Poutrel[§]

* Institut de Mécanique des Fluides de Toulouse, 1 Allée du Professeur Camille Soula, 31400 Toulouse, France. Email: ababou@imft.fr (*corresponding author*)

† Institut de Radioprotection et de Sûreté Nucléaire (IRSN), Laboratoire LRSS, 31 Avenue du Général Leclerc, 92260 Fontenay-aux-Roses, France

§ ANDRA, Direction Scientifique / Mécanique des Fluides et des Solides, Parc de la Croix Blanche - 1/7 rue Jean Monnet, 92298 Châtenay-Malabry, France

Key words: Porous media, randomly heterogeneous media, fractured porous media, desaturation, unsaturated permeability, upscaling, power average, non linear anisotropy.

Summary. This paper presents results of numerical simulations and upscaling for unsaturated flow in randomly heterogeneous and stratified samples (permeametric and gravimetric flow "experiments"). The aim is to upscale numerically the nonlinear unsaturated permeability (Kii) *vs.* capillary pressure or suction (Ψ), and to compare the resulting Kii(Ψ) curve to a statistical Power Average (PA) theory, taking into account nonlinear anisotropy. The behavior of the PA exponent (ωi) is studied in terms of capillary/geometric length scales. The implications of this work for fractured porous media are discussed. The final objective is to use the upscaled Kii(Ψ) curve for studying drying phenomena, or desaturation and decompression fronts, in the damaged zone around the walls of ventilated galleries and other excavations at ANDRA's Bure URL (Underground Research Laboratory).

1 INTRODUCTION

This paper presents results of numerical upscaling "experiments" for unsaturated flow on randomly heterogeneous and stratified samples. The multiple simulations are aimed at upscaling numerically the nonlinear unsaturated permeability (Kii) *vs.* capillary pressure or suction (ψ). The upscaled results Kii(Ψ) are then compared to a statistical power averaging theory, taking into account the nonlinear anisotropy of Kii(Ψ). The behavior of the power exponent is studied in terms of capillary/geometric length scales, and the implications of this work for fractured porous media are discussed.

This basic research is part of investigations conducted by ANDRA (Agence Nationale de gestion de Déchets RAdioactifs) on the isolation properties of a claystone geologic repository for radioactive waste, including in particular theoretical and numerical studies on the upscaled

hydraulic and hydro-mechanical behavior of fissured/fractured claystone around underground galleries at the Bure URL (Underground Research Laboratory).

Previous studies [1] have focused on the upscaled saturated hydraulic conductivity tensor Kij, which was obtained explicitly in terms of the geometrical structure of fissures (statistical set) and of large curved fractures (deterministic set), based on a flux superposition method (frozen gradient approximation). However, in this paper, we are interested in unsaturated flow. The immediate objective is to capture the behavior of the upscaled unsaturated permeability as a function of suction and flow direction (anisotropy). The final objective is to use the upscaled Kii(Ψ) to model drying and (possibly) re-saturation phenomena in the damaged zone around excavations (ventilated galleries).

2 THEORY FOR UPSCALED K(Ψ) CURVE (PROBABILISTIC POWER AVERAGE)

The work is based on a previously developed theoretical nonlinear Power Average model for the upscaled Kii(Ψ) curve, with explicit results in the case of random media, and in particular, randomly stratified media [3], [4]. The resulting theoretical curve Kii(Ψ) depends on the variability and structure of the porous medium, and on a directional power exponent (ωi) to be determined. This work focuses on the case where the local permeability of the random medium can be described by the exponential Gardner model (**eq.1a**) with spatially correlated & cross-correlated coefficients (lnKs(**x**), β(**x**)). Then, considering the probabilistic power average (**eq.1b**):

$$(a):\ K(\psi;\mathbf{x}) = K_S(\mathbf{x})\exp\{-\beta(\mathbf{x})\psi\} \qquad (b):\ \hat{K}_{ii}^{PA}(\psi) = \left\langle K(\psi;\mathbf{x})^{\omega_i}\right\rangle^{1/\omega_i} \qquad (1a,\ 1b)$$

the following explicit result was obtained in reference [3] (an extension of Mualem's model [6]):

$$\hat{K}_{ii}^{PA}(\Psi) = K_G \exp[-\Psi]\exp\left[\frac{1}{2}\,\omega_i\left(\frac{\sigma_\beta^{\,2}}{\langle\beta\rangle^2}\,\Psi^2 - 2\,\rho\,\frac{\sigma_\beta}{\langle\beta\rangle}\sigma_{\ln K_S}\,\Psi + \sigma_{\ln K_S}^2\right)\right] \qquad (2a)$$

$$\Leftrightarrow \hat{K}_{ii(ABC)}^{PA}(\Psi) = \exp\left[\frac{1}{2}\left(A\,\Psi^2 - B\,\Psi + C\right) - \Psi\right] \qquad (2b)$$

where "Ψ" represents the mean dimensionless suction $\Psi = \beta_G\langle\psi\rangle$, with $\beta_G \approx \langle\beta\rangle$ in practice.

The form of **eq.2b** is just another manner of expressing the same result with three coefficients (A,B,C). For a homogeneous medium we get (A,B,C)=(0,0,0) and the upscaled curve coïncides with the local exponential curve. Other parameters in **eq.2a** are the standard deviations (σ) of random fields β(x) and lnKs(**x**), the geometric mean K_G of Ks(**x**), and the cross-correlation ρ between ((lnKs(**x**), β(**x**)).

Our literature review (*not shown here for lack of space*) indicates, from field data, that the cross-correlation ρ is significant and positive for heterogeneous sedimentary soils ($+0.70 \le \rho \le +1.00$). Furthermore, this is confirmed by a simple capillary model of flow in a statistical fracture network, as pointed out in reference [7] (*Section 4.4, Eq.4.64: some equations there were given without dimensional factors; this is now fixed below)*. Specifically, considering

$\beta(\mathbf{x})$ as a scaling factor in the permeability curve, it was found that, in the presence of a statistical network of unsaturated parallel plate fractures [7]:

$$\beta(\mathbf{x}) \approx \frac{\rho g}{\sigma_{SURF}} \sqrt{\frac{k(\mathbf{x})}{\phi(\mathbf{x})}} = \frac{\rho g}{\sigma_{SURF}} \sqrt{\frac{\nu}{g} \frac{K_S(\mathbf{x})}{\theta_S(\mathbf{x})}} \tag{3}$$

where k is Darcy permeability (m^2), ϕ is porosity due to fractures, σ_{SURF} is surface tension (N/m). Usually porosity varies much less than permeability. It is concluded that the unsaturated scaling factor $\beta(\mathbf{x})$ tends to be positively correlated to $Ks(\mathbf{x})$ or $\ln Ks(\mathbf{x})$: $0 < \rho \leq 1$. Let us test **eq.3** by applying it for a fine grained medium with $\theta s \approx 0.40$ and $Ks \approx 1E\text{-}6 m/s$: this yields $1/\beta \approx 0.15$ m capillary length scale; decreasing Ks by a factor 100 yields $1/\beta \approx 1.5$ m (all reasonable values).

Finally, the remaining parameter to be discussed in **eq.2** is the directional PA exponent "ωi", to be determined. The special values $\omega = +1, 0, -1$, when inserted in **eq.2**, yield the arithmetic, geometric, and harmonic mean permeability curves, respectively.

In the *Mualem* model, the value $\omega = +1$ is used for flow parallel to layers, and $\omega = -1$ for flow orthogonal to layers (with these values, **eq.2** yields explicitly the permeability curves corresponding to a statistical version of *Mualem*'s model).

However, we will see below that the arithmetic/harmonic curves do not fully account for capillary effects, whence the need to investigate other values for ω. Previous numerical investigations [4, 5] have indicated that (ωi) does not only depend on flow direction with respect to strata, but also on the mean $<\beta>$ which represents an inverse capillary length scale. The relation between (ωi) and $<\beta>$ was conjectured, but it was clear that more extensive simulations were needed to confirm these indications and to capture the behavior of (ωi).

3 NUMERICAL UPSCALING

We now present briefly a set of numerical experiments designed for that purpose. After obtaining the upscaled $Kii(\Psi)$ numerically, the aim is to compare it with the theoretical $Kii(\Psi)$ of **eq.2** in order to identify the best fitted directional exponent (ωi), and to study its behavior depending on the structure of the medium.

3.1 Numerics

The numerical experiments were conducted as follows. The heterogeneous samples were generated on a high resolution grid using the turning band random field generator [8]. Two types of "experiments" & boundary conditions were defined: permeametric & gravimetric (unsaturated in both cases)[1]. On each sample, dozens of transient flow experiments were conducted in order to obtain the final steady flux & the mean suction "Ψ" in the sample. Darcy's law was then applied to obtain the macro-scale curve $Kii(\Psi)$ for the specified flow direction "ii" (e.g., K_{XX} or K_{ZZ}).

The numerical tests were conducted using the Implicit Finite Volume BIGFLOW 3D-Python code, solving numerically a generalized version of Richards equation for partially

[1] Most results were obtained with unsaturated permeametric experiments. In some cases, however, it was verified that gravimetric & permeametric experiments yield the same upscaled $K(\Psi)$ curves (vertical flow orthogonal to strata).

saturated/unsaturated flow in heterogeneous media (with Preconditioned Conjugate Gradients and Fixed Point / Modified Picard iterations) [9]. The code was enhanced with an additional Python layer (MULTISIM) to launch multiple simulations for many different boundary conditions, while keeping a control on mass balance & convergence to steady state.

Each "experiment" provides only one point (K_n, Ψ_n) on the upscaled Kii(Ψ) curve. Briefly, K_n is calculated from the numerical flux/gradient ratio, and Ψ_n is the volume average of $\psi(\mathbf{x})$, at the scale of the sample. Each curve required about 10 to 20 experiments. In total, hundreds of unsaturated flow simulations were launched and analyzed.

3.2 Simulation results on randomly heterogeneous samples

We show briefly in **Figure 1** just a few examples of heterogeneous samples on which unsaturated flow experiments were conducted.

We also show in **Figure 2** (*further below*) a set of multiple transient flow experiments (converging to steady state) for the randomly stratified sample, with vertical flow orthogonal to strata induced by unsaturated permeametric boundary conditions [2]. The figure shows intermediate transient pressure profiles during the sequential multi-simulation procedure. Internal ponding phenomena can be seen to occur for this particular experiment [3].

3.3 The numerically upscaled Kii(Ψ) curves

As mentioned earlier, the numerically upscaled Kii(Ψ) curves are constructed point-by-point (K_n, Ψ_n). In some cases, under relatively "wet" flow regimes, internal saturation and ponding could occur and remain stable at steady state: this is an interesting phenomenon (not covered by the various upscaling theories known to us). We choose to show here (**Figure 3**) an example of a numerically constructed curve where the "saturation/ponding" phenomenon did occur at low values of mean suction (see the rectangular frame in **Figure 3**).

It now remains to be seen how such curves compare to the PA theory, and what is the best fitted value of (ωi) in different cases: this is the object of the next section.

4 OPTIMIZATION OF POWER EXPONENT (FITTING PROCEDURE &RESULTS)

4.1 Optimization approach for fitting the Power Average exponent ω

The problem now is to obtain, for each numerically upscaled curve Kii(Ψ), the best fitted non linear Power Average curve (**eq.2a** or **eq.2b**). We used a least square optimization method implemented in MATLAB (function *lsqnonlin* with Levenberg-Marquardt). We have tested four different formulations for the optimization problem, from the following two pairs of choices: **(i)** optimizing the three parameters (A,B,C) *vs.* optimizing the single PA exponent (ω); **(ii)** performing the least square fit in terms of K(Ψ) *vs.* in terms of lnK(Ψ).

[2] Note: (a) similar flow results were obtained for vertical flow under gravimetric conditions; (b) other simulations not shown here included horizontal flow parallel to strata, and 2D (x, z) flow in random imperfectly stratified samples.

[3] Note: the final steady state used for K(Ψ) upscaling still has some ponded zones, although much less so.

Briefly, we choose to focus on the optimal fit of the single PA exponent (ω) in terms of lnK. In fact, the optimal fit was usually better with (A, B, C) than with the single (ω), as it should. In spite of this, we choose to fit the single parameter (ω) because we prefer **eq.2a** for theoretical reasons (the heterogeneous structure of the medium appears explicitly, along with ω, in **eq.2a**). Secondly, we have found differences in the (ω) fitted in terms of K(Ψ) *vs.* lnK(Ψ). The lnK fit was finally chosen because it provides a better fitted curve over a broader range of suctions. This choice is also based on the fact that, considering all test cases, the behavior of the fitted exponent (ω) obtained with lnK(Ψ) seemed more consistent than that obtained with K(Ψ).

4.2 Optimization results: the fitted Power Average exponent ω

Table 1 below summarizes the best fitted values of the PA exponent (ω) obtained for the vertical flow experiments in the randomly stratified samples with mean flow orthogonal to strata[4]. The different columns correspond to different values of the mean β and, equivalently, of the capillary ratio μ_{CAP} to be defined below. Ks(z) is a spatially correlated random field, β(z) is perfectly cross-correlated to Ks(z) in the first column, or constant in the other columns.

	1D ⊥ (flow // Oz)	1D ⊥ (flow // Oz)	1D ⊥ (flow // Oz)	1D ⊥ (flow // Oz)	1D ⊥ (flow // Oz)	1D ⊥ (flow // Oz)
β	$\langle\beta(z)\rangle$ = **8.133**	**0.640**	**1.60**	**8.133**	**40.000**	**100.000**
μ_{CAP}	**0.8133**	**0.064**	**0.160**	**0.8133**	**4.000**	**10.000**
Power **ω**	**-4.478E-01**	**-6.368E-01**	**-3.978E-01**	**-4.882E-02**	**+2.001E-01**	**+3.388E-01**

Table 1: Optimal values of ω obtained by fitting the Power Average model to the numerically upscaled K(Ψ) curves [ln(K) fit]. Note: $\mu_{CAP} = \lambda_{HET}.\beta = \lambda_{HET}/\lambda_{CAP}$ where $\lambda_{CAP} = 1/\beta$, and λ_{HET} is the correlation scale in the direction of flow (thus $\lambda_{HET}=\lambda_X$ if flow // Ox, or $\lambda_{HET}=\lambda_Z$ if flow // Oz as here).

5 BEHAVIOR OF POWER EXPONENT *VS.* CAPILLARY/GEOMETRIC SCALES

Recall that the numerical experiments on heterogeneous samples were used to obtain upscaled unsaturated Kii(Ψ) curves described point by point. The Power Average exponent "ωi" was then identified by a best fit procedure. The results are now used to confirm a previously formulated conjecture concerning the behavior of the Power Average exponent "ωi" *vs.* capillary effects.

[4] Other results not shown and not discussed here.

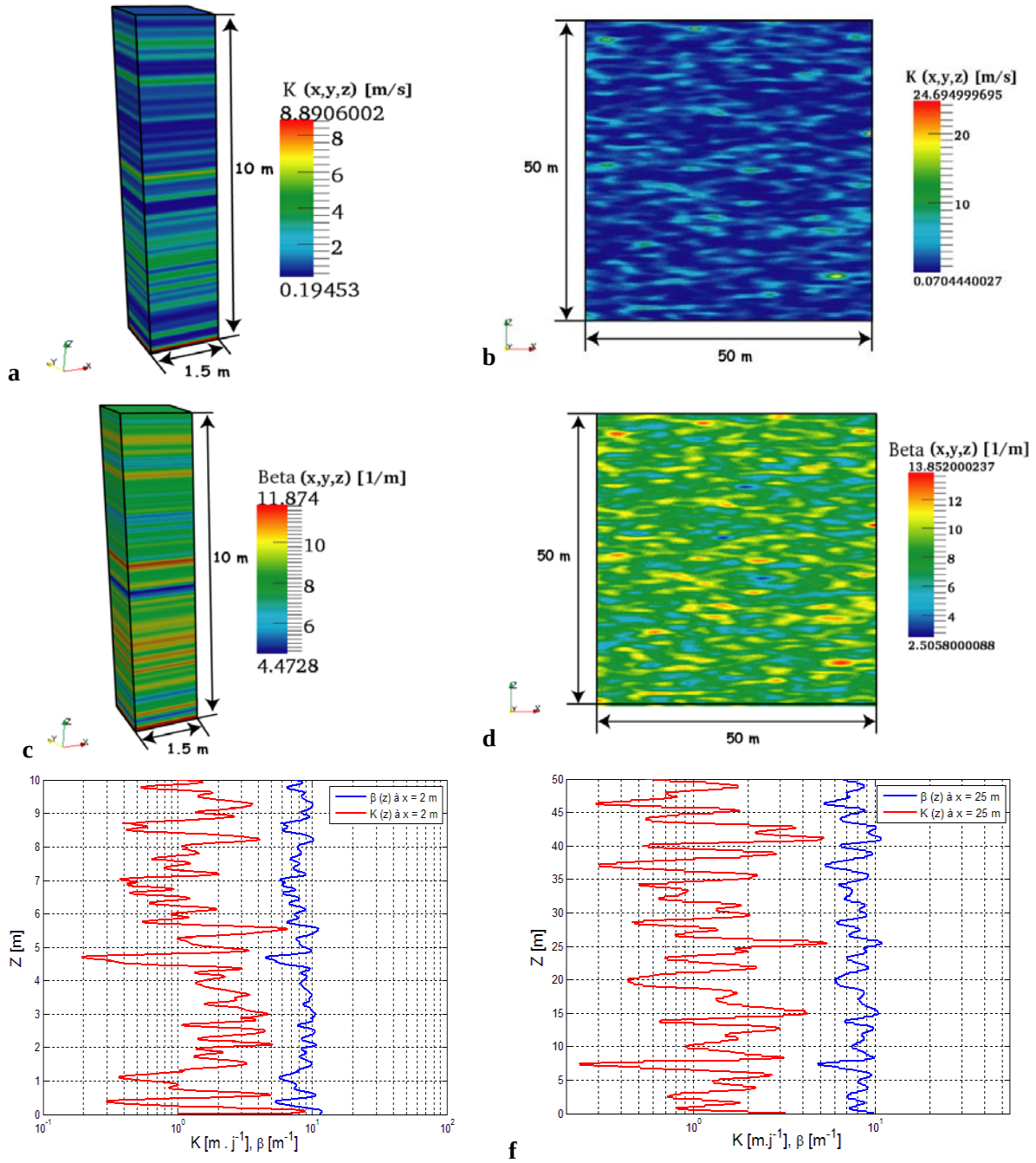

Figure 1: Random permeability field Ks(x,y,z) [m/day]: **(a)** perfectly stratified medium, and **(b)** imperfectly stratified medium. Random field β(x,y,z) [1/m]: **(c)** perfectly stratified medium, and **(d)** imperfectly stratified medium. Comparisons of vertical profiles of Ks(z) and β(z) at x = 2 m **(e)** and x = 25 m **(f)** in the 2D medium. Note: in both 1D and 2D samples, here, β is perfectly cross-correlated to Ks.

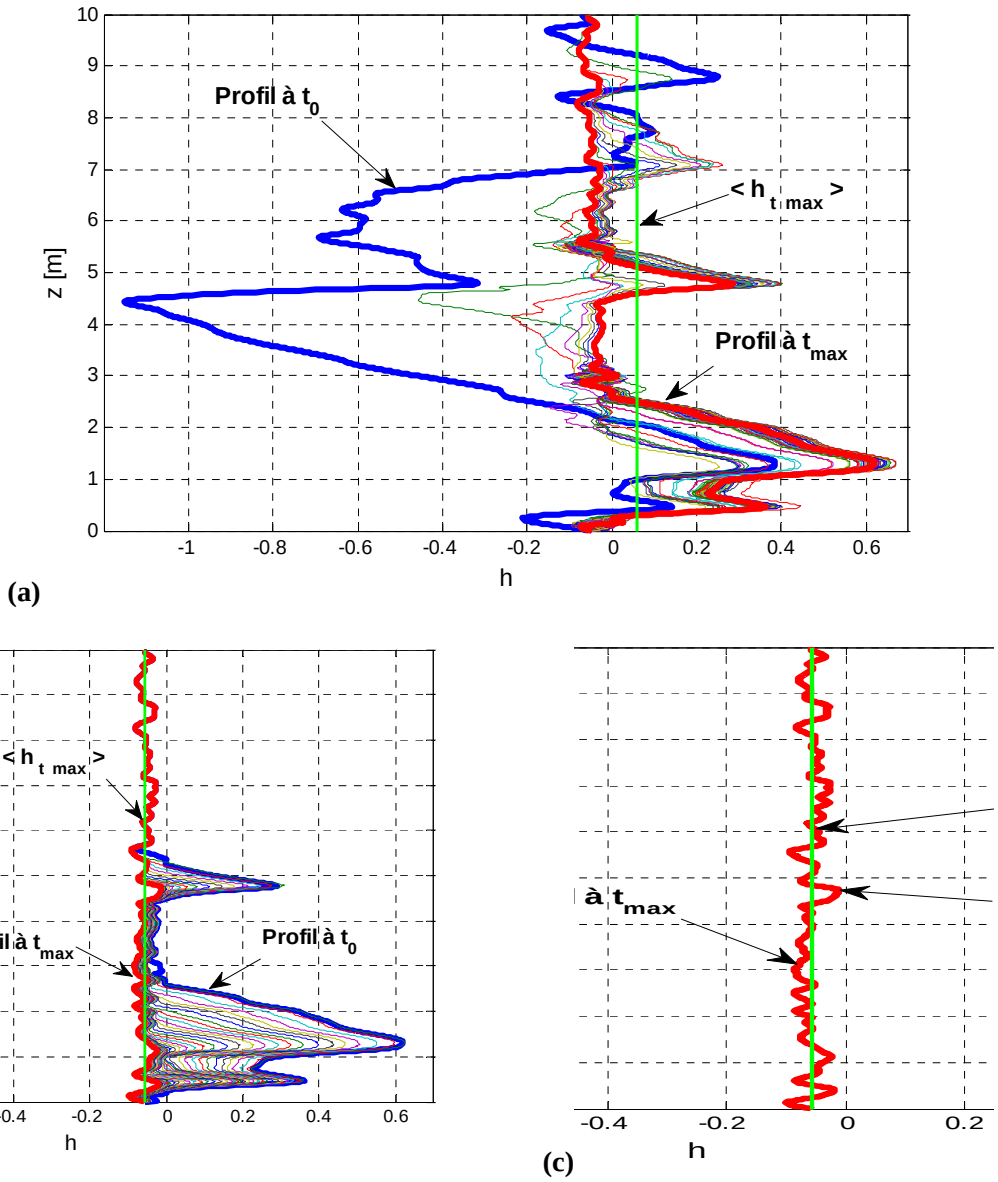

Figure 2: Transient numerical simulations: evolution of vertical pressure profiles h(z,t), along the mean flow direction (permeametric test with flow orthogonal to layers). Each graph shows the profiles h(z) between an "initial" time **t0** (**blue**) and a "max" time **tmax** (**red**) for one "iteration" of the sequential MULTISIM algorithm. **(a)** Simulated profiles at the end of the first iteration of MULTISIM; **(b)** second iteration of MULTISIM; and **(c)** third iteration of MULTISIM (the steady state is reached - the next step is to perform the upscaling).

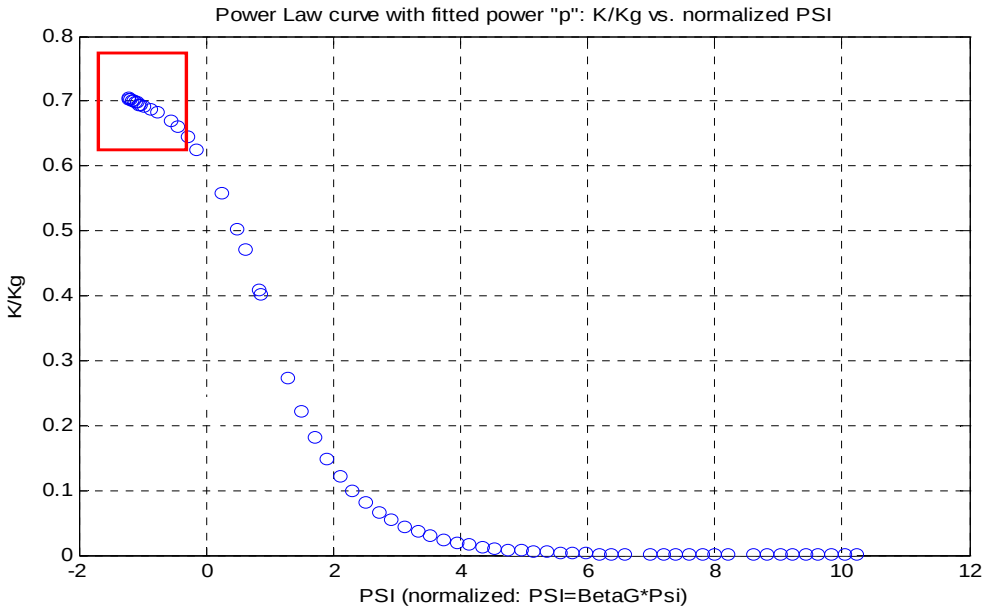

Figure 3: Numerically upscaled conductivity curve $K_{ZZ}(\Psi)$ for 1D vertical flow orthogonal to strata. Parameters: lnKs is randomly stratified with vertical correlation scale $\lambda_Z = 0.10$ m and standard deviation $\sigma(\ln Ks) = 0.771$; β is constant here, and equal to 8.133 m^{-1} (capillary length scale $1/\beta = 0.13$ m). The curve is presented in dimensionless variables: K/K_G where $K_G \equiv \exp(<\ln Ks>)$, and $\Psi \equiv \beta.<\psi>$ or $\Psi \equiv <\beta>.<\psi>$ more generally when β is variable. Each point (symbol "o") represents the steady state solution of a flow simulation experiment. The red rectangle indicates the results obtained in the "wet" flow regime with internal ponding in some regions (this is the reason for the mean suction being negative although the sample is not fully saturated). The unsaturated upscaling theory only addresses the part of the curve where Ψ is significantly positive.

Basically, we seek a formulation of the (fitted) "ωi" in terms of a capillary/geometry scale ratio which characterizes the heterogeneous unsaturated medium. Accordingly, the fitted exponent "ω" "was studied as a function of a dimensionless capillary ratio μ_{CAP} defined as follows (we write "μ_{CAPii}" because of the dependence on flow direction "i"):

$$\mu_{CAP\mathbf{ii}} = \lambda_{HET\mathbf{ii}}\,\beta \approx \lambda_{HET\mathbf{ii}} / \lambda_{CAP} \tag{4}$$

This capillary ratio, μ_{CAP}, can be interpreted as the ratio of a geometric scale of heterogeneity (here a characteristic layer thickness) *versus* a capillary length scale λ_{HET} (here represented by $1/<\beta>$). The capillary ratio is directional because the geometric heterogeneity length scale is directional (λ_{HET}. caracterizes heterogeneity along the direction of mean flow). Following these ideas, the results of **Table 1** are plotted in **Figure 4** as $\omega^{OPT}=f(\mu_{CAP})$.

Furthermore, the numerical relation $\omega=f(\mu_{CAP})$ is rather well fitted by the analytical function:

$$\omega_{ii} = f\left(\mu_{CAP\mathbf{ii}}\right) \approx \frac{2\left(\mu_{CAP\mathbf{ii}}\right)^{1/3}}{1+\left(\mu_{CAP\mathbf{ii}}\right)^{1/3}} - 1 \tag{5}$$

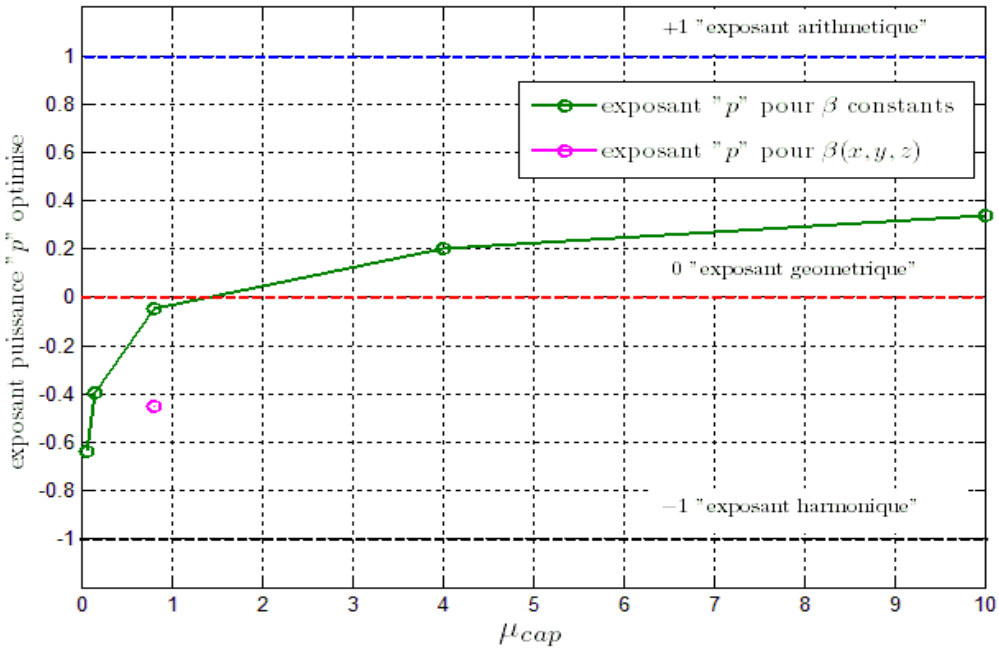

Figure 4: Optimal Power Average exponent "ω", fitted in terms of lnK, and plotted as a function of the capillary ratio μ_{CAP} defined in the text: $\omega = f(\mu_{CAP})$. Each point represents a numerical flow experiment on the randomly stratified sample (here, flow is orthogonal to strata). The **green curve** shows results for β constant in space. The isolated point "**o**" corresponds to β random and perfectly cross-correlated to Ks. The ordinate value ω = 0 corresponds to the geometric mean K(Ψ) curve, the lower "bound" ω= -1 to the harmonic mean K(Ψ) curve, and the upper "bound" ω= +1 to the arithmetic mean K(Ψ) curve.

It is important to note that the behavior of the upscaled unsaturated permeability curve depends not only of flow direction and on layer thickness, but also at the same time on $\lambda_{CAP}=1/\beta$. For $\mu_{CAP} \approx 1$ ($\lambda_{HET} \approx \lambda_{CAP}=1/\beta$) we obtain an exponent $\omega \approx 0$, and therefore, the upscaled permeability curve is the geometric mean curve (even though the medium is stratified). The harmonic mean curve appears only as an asymptotic case for $\mu_{CAP} \to 0$ (our smallest negative exponent was in fact ω≈-0.64). And finally, the arithmetic mean curve appears as an asymptotic case for $\mu_{CAP} \to \infty$ (our largest positive exponent was in fact ω≈+0.34).

These results can be explained as follows: **(i)** if $\mu_{CAP} \ll 1$, then $\lambda_{HET} \ll \lambda_{CAP}$, and any capillary region of diameter λ_{CAP} will contain many layers (whence the harmonic behavior); **(ii)** if $\mu_{CA} \gg 1$, then $\lambda_{HET} \gg \lambda_{CAP}$, and any capillary region of diameter λ_{CAP} will contain only one piece of a layer (whence the arithmetic behavior).

Finally, if the behavior of the Power Average exponent is known, the power average model of **eq.2a** can be transposed to other random media structures, such as a Matrix/Fracture medium with binary (Bernoulli) permeability distribution. Briefly, given "ωii", the upscaled "Power Average" permeability-suction curve of the Matrix/Fracture medium is given by:

$$\frac{\hat{K}_{ii}^{PA}(\Psi)}{K_M(\Psi)} = \begin{cases} \left\{ \Phi \left(\frac{K_F(\Psi)}{K_M(\Psi)} \right)^{\omega_i} + (1-\Phi) \right\}^{1/\omega_i} & (\omega_i \neq 0) \\ \left(\frac{K_F(\Psi)}{K_M(\Psi)} \right)^{\Phi} & (\omega_i = 0) \end{cases} \quad (6)$$

where K_F and K_M are respectively the unsaturated permeability curves characterizing the "fracture" and "matrix" media, and Φ is the volumetric fraction of the "fracture" system.

11 CONCLUSIONS AND OUTLOOK

The upscaled permeability-suction curve was analyzed with a nonlinear Power Average model, which accounts for structure, variability, and flow direction (anisotropy). The resulting Kii(Ψ) curve is non linearly anisotropic. The model depends on a power exponent "ωii". The behavior of "ωii" was studied with multiple flow experiments on randomly stratified media (and other structures). It was found that the best fitted power ωii increases with a capillary/geometric scale ratio (μ_{CAPii}). These findings need to be extended to a variety of other structures. For a given "ωii", the PA model can be readily expressed for the case of binary matrix/fracture media.

REFERENCES

[1] R. Ababou, I. Canamon, A. Poutrel: Macro-Permeability Distribution and Anisotropy in a 3D Fissured and Fractured Clay Rock: 'Excavation Damaged Zone' around a Cylindrical Drift in Callovo-Oxfordian Argilite (Bure). Special Issue "Clays in Natural & Engineered Barriers for Radioactive Waste Confinement" (4th Internat. Meet. Clays 2010, Nantes, March 29–April 1, 2010). *J. of Physics & Chemistry of the Earth*, ISSN:1474-7065, DOI:10.1016/ j.pce.2011.07.032, (2011).

[3] R. Ababou, "Probabilistic Analysis of Unsaturated Conductivity: Anisotropy, Crossing Point, and Upper Envelope", Chapter 6: Stochastic Analysis of Flow and Transport (Section 6.3) in : Report on Research Activities for Calendar Year 1991, NUREG/CR-5817 & CNWRA 91-01A, W.C. Patrick (ed.), U.S. Nuclear Regulatory Comm., Government Printing Office, Washington DC (1993).

[4] A.C. Bagtzoglou, S. Mohanty, A. Nedungadi, T.-C.J. Yeh and R. Ababou, "*Effective Hydraulic Property Calculations for Unsaturated, Fractured Rock with Semi-Analytical and Direct Numerical Techniques: Review and Applications"*. Report CNWRA 94-007, Monographic Series ISSN 1547-3023, San Antonio, Texas: Southwest Research Institute, March 1994, 8 chapters, 168 pp. (1994).

[5] V.S. Soraganvi, R. Ababou and M.S. Mohan Kumar, "Modeling and Upscaling Unsaturated Flow through Randomly Heterogeneous Soils". CMWR'2010, Barcelona, Spain, 21-24 June, XVIIIth Internat. Conf. *Comput. Meth. in Water Resour.* ("Stochastic Hydrology"): Paper 212, 10 pp., (2010).

[6] Y. Mualem, "Anisotropy of unsaturated soils". *Soil Sci. Soc. Am. J.*, 48, 505-509 (1984).

[7] R. Ababou, "*Approaches to Large Scale Unsaturated Flow in Heterogeneous, Stratified, and Fractured Geologic Media*". Report NUREG/CR-5743, U.S. Nuclear Regulatory Comm., Government Printing Office, Washington DC, 150 pp., (1991).

[8] A.F.B. Tompson, R. Ababou and L.W. Gelhar, "Implementation of the Three-Dimensional Turning Bands Random Field Generator." *Water Resources Research*, 25(10), 2227-2243 (1989).

[9] Ababou R., B. Sagar, G. Wittmeyer (1992): Testing Procedures for Spatially Distributed Flow Models. *Advances in Water Resources*, Vol. 15, pp. 181-198, 1992.